Reinforced Concrete Response to Simulated Earthquakes

T. Takeda[1]
M. A. Sozen[2]
N. N. Nielsen

1. INTRODUCTION

The response analysis of reinforced concrete structures subjected to strong earthquake motions requires a realistic conceptual model which recognizes the continually varying stiffness and energy-absorbing characteristics of the structure. Such a model is proposed in this paper and its applicability to reinforced concrete is tested experimentally with the use of specimens subjected to dynamic base motions, generated by the University of Illinois Earthquake Simulator. The spectral responses, based on the proposed characteristics of the structure, are calculated and discussed.

2. THE TEST SPECIMEN AND TEST PROCEDURES

The dimensions and reinforcing arrangement are shown in Fig. 2. The static yield stress was 51,000 psi for the main reinforcement and 40,000 psi for the transverse reinforcement. Five specimens were tested, two of which were subjected to simulated earthquakes.

As shown in Fig. 1, two steel masses of 2015 lbs. were hung on each side of the specimen on a one-in. steel shaft resting on ball bearings. To restrain large rotations of the steel mass, two 0.25-in. round prestressed rods tied the mass to the platform (Fig. 1).

3. PROPOSED STATIC RESPONSE

The static response was idealized by defining a "Primary curve" for initial loading and a set of rules for reversals as described in the next two section.

The Primary Curve

Three linear segments in each quadrant define the primary curve (Fig. 3a). The first break in the curve refers to cracking. The coordinates of this point (Pcr, Dcr) were computed routinely with the concrete flexural tensile strength assumed to be 530 psi.

The yield load, Py, was obtained assuming a parabolic compressive stress-strain curve for the concrete. The yield deflection, Dy, was the sum of four parts: (1) deflection caused by curvature based on cracked section, (2) deflection caused by slip of the reinforcement and depression of the concrete at the beam-column interface. (3) deflection caused by deformation of the test platform, and (4) the shearing deflection. To determine part (2) it was assumed that the anchorage bond at yielding of the bar extended uniformly over 20 bar diameters. The depression of the concrete was calculated by treating the horizontal beam as a "semi-infinite plate" (Ref. 1).

---

[1] Manager of Structural Engineering Laboratory, Technical Research Institute, OHBAYASHI-GUMI, LTD., Tokyo, Japan
[2] Professor of Civil Engineering, University of Illinois, Urbana, Illinois
[3] Professor of Civil Engineering, University of Hawaii Honolulu, Hawaii

The relative contributions of the four parts to the total deflection were: part 1, 56%; part 2, 31%; part 3, 11%, part 4, 2%. The slope of the third segment of the primary curve was calculated to be about 1/100 of elastic rigidity.

Concrete properties assumed in determining the primary curve were the following. Compressive strength: 4400 psi. Modulus of rupture: 530 psi. Young's modulus: 3.6×10^6 psi.

Response Under Load Reversals

There are many possible alternatives at each point in the loading history. Rules are given for loading and unloading for different conditions and illustrated in Fig. 3b and 3c.

1). *Condition:* The cracking load, Pcr, has not been exceed in one direction. The load is reversed from a load P ($P<Py$) in the other direction.

Rule: Lnloading follows a straight line from the position at load P to the point representing the cracking load in the other direction.

Example: Segment 3 in Fig. 3b (If unloading occurs before deformations represented by segment 2, the rules provide no hysteresis loop.)

2). *Condition:* A load P_1 is reached in one direction on the primary curve such that $Pcr<P_1<Py$. The load is then reversed to $-P_2$ such that $P_2<P_1$.

Rule: Unload parallel to laoding curve for that half cycle.

Example: Segment 5 parallel to segment 3 in Fib. 3b.

3). *Condition:* A load P_1 is reached in one direction such that $P_{cr}<P_1<P_r$. The load is then reversed to $-P_3$ such that $P_3>P_1$.

Rule: Unloading follows a straight line joining the point of return and the point representing cracking in the other direction.

Example: Segment 10b in Fig. 3b.

4). *Condition:* One or more loading cycles have occurred. The load is zero.

Rule: To construct the loading curve, connect the point at zero load to the point reached in the previous cycle, if that point lies on the primary curve or on a line aimed at a point on the primary curve. If the previous loading cycle contains no such point, go to the preceding cycle and continue the process until such a point is found. Then connect that point to the point at zero load.

Exception: If connecting the point at zero load to the yield point on the primary curve results in a higher slope, use that line as the loading curve.

Examples: Segment 12 in Fig. 3b represents the exception. It is aimed at the yield point rather than at the highest point on segment 2. Segment 8 in Fig. 3b represents a routine application, while segment 20 represents a case where the loading curve is aimed at the maximum point of segment 12.

5). *Condition:* The yield load, P_y, is exceeded in one direction.

Rule: Unloading curve follows the slope given by the following expression adapted from Reference 2.

$$k_r = k_y (D_y/D)^{0.4}$$

where k_r = slope of unloading curve

k_y = slope of a line joining the yield point in one direction to the cracking point in the other direction

D = maximum deflection attained in the direction of the loading

D_y = deflection at yield

Example: Segment 4 in Fig. 3c.

6). *Condition:* The yield load is exceeded in one direction but the cracking load is not exceeded in the opposite direction.

Rule: Unloading follows Rule 5. Loading in the other direction continues as an extension of the unloading line up to the cracking load. Then, the loading curve is aimed at the yield point.

Example: Segments 4 and 5 in Fig. 3c.

7). *Condition:* One or more loading cycles have occurred.

Rule: If the immediately preceding quarter-cycle remained on one side of the zero-load axis, unload at the rate based on rules 2, 3, or 5, whichever governed in the previous loading history.

Example: Segment 7 in Fig. 3b.

4. SIMURATED EARTHQUAKE MOTIONS

Three tests were run with the motion of the platform designed to simulate various earthquake motions. The main characteristics of the platform motions are described in the following sections.

Run 11: In run 11, the displacement record for the N-S component of the El Centro 1940 earthquake was fed into the command center of the actuator such that 40 seconds of the original earthquake record were played through in 5 seconds. The maximum platform acceleration was measured to be 1.28G and the maximum platform displacement was 1.2 in. The measured platform acceleration is shown in Fig. 4a.

Run 12: In this run, the original EL Centro 1940 N-S tape was compressed 16 times resulting in a maximum acceleration of 2.4G. The maximum displacement was 0.88 in. The platform acceleration record is shown in Fig. 5a.

Run 21: This run was patterned after the N21E component of Taft 1952. The time was compressed by a factor of 10 while the maximum acceleration was increased to 2.7G (Fig. 6a).

5. RESPONSE TO SIMULATED EARTHQUAKE MOTIONS

The measured and calculated response of the mass attached to the specimen in test runs 11, 12 and 21 are shown in Fig. 4, 5 and 6. Maximum values are summarized in Table 1.

Acceleration measurements were made on both the north and south faces of the mass. These measurements differed by very small amounts indicating that the torsion of the mass was negligible.

The response at the centroid of the mass to the simulated earthquake motions was calculated using a step-by-step numerical integration method. The acceleration was assumed to vary linearly over intervals of 0.002 sec. while the integration step was 0.0004 sec. The static force-deflection relationship of the reinforced concrete specimen was programmed in accordance with the rules described earlier in the paper. Run 12 was conducted with specimen T2 after the same specimen had already been subjected to run 11. In the analysis, runs 11 and 12 were treated continuously. However, after the base motion for run 11 was terminated, the acceleration and the velocity of the mass were made zero.

The response was calculated for no damping and for an equivalent viscous damping equal to two percent of the critical.

The main effect of the assumed damping was on the calculated maximum displacements. The measured maximum accelerations exceeded the calculated values (Table 1). The measured strain rate in the reinforcement approached 0.1 per second, a rate which would justify an increase in the steel yield stress, and therefore in the calculated acceleration, by 20 percent. Maximum displacements calculated for $h = 0$ compared better with the measured values than those based on 2% daming.

In general, the measured and calculated response histories compared very favorably. But the proposed hysteresis has tendency to give larger energy absorption characteristics in the portion of weak excitation.

6. SPECTRAL RESPONSE

Spectral response, based on the proposed hysteresis, to EL CENTRO 1940 NS and to TAFT 1952 NS are shown in Fig. 7, in which yield acceleration was set at 0.2G, cracking acceleration at 0.05G and yield displacement was twice as that of elastic.

Although it is questionable whether the characteristics can be applicable in the range of large displacement, according to the response spectra to EL CENTRO, it is certain that much more attention should be given in the design of the structure with short natural period. The response spectra has tendency to give larger displacement than that of elastic or elasto-plastic hysteresis, especially in shorter natural period.

7. CONCLUSIONS

1) Dynamic response calculated on the basis of the proposed force-displacement relationship resulted in satisfactory agreement with the measured response at all levels of excitation during the tests with earthquake motions.

2) With the hysteresis loops defined by the proposed force-displacement relationship, it was not necessary to invoke additional sources of energy absorption for a satisfactory prediction of the dynamic response.

3) The spectral response to EL CENTRO, based on the proposed hysteresis ($Qy = 0.2G$, $Qc = 0.05G$, $Ty = \sqrt{2}\,Te$), shows large displacement in the structure with short natural period.

8. ACKNOWLEDGEMENTS

The University of Illinois Earthquake Simulator was acquired under equipment grant GK 980 by the U. S. National Science Foundation. The reported work was carried out at the Structural Research Laboratory of the University of Illinois under NSF research grant GK 1118X.

Acknowledgment is due V. J. McDonald, Associate Professor of Civil Engineering, and P. Gulkan, F. Imbeault, E. Perry and S. Otani, graduate students in civil engineering, for their contributions to the execution and analysis of the tests.

9. APPENDIX I—REFERENCES

1. Timoshenko, S., and Goodier, J. N. "Theory of Elasticity", McGraw-Hill, 1951, p. 96.
2. Takeda, T., "Study of the Load-Deflection Characteristics of Reinforced Concrete Beams Subjected to Alternating Loads (In Japanese)", Transactions, Architectural Institute of Japan, Volume 76, September 1962.
3. Takeda, T., Sozen, M. A., Nielsen, N. N. "Reinforced Concrete Response to Simulated Earthquakes", Jounal of the Structural Div. Proceeding of the American Society of Civil Engineers Dec. 1970 p. 2257.

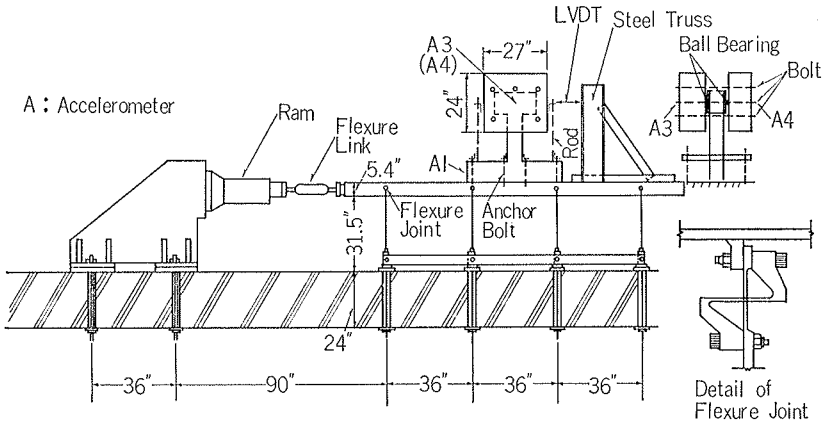

Fig. 1 The University of Illinois Earthquake Simulator with the Test Sepcimen in Place

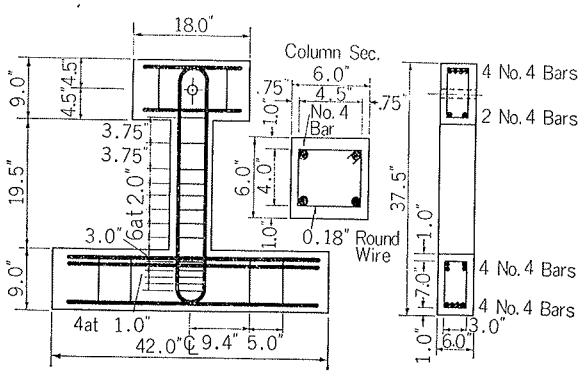

Fig. 2 The Test Specimen

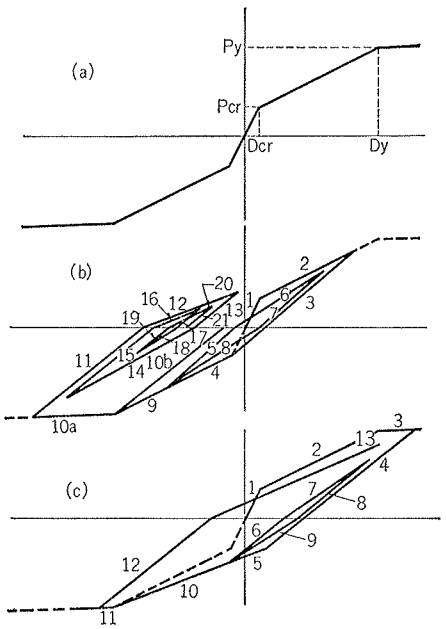

Fig. 3 Load Deflection Curves

	Run 11 (Test Specimen T2)				Run 12 (Test Specimen T2)				Run 21 (Test Specimen T5)			
	Acceleration		Displacement		Acceleration		Displacement		Acceleration		Displacement	
	East	West	East	West	East	West	East	West	East	West	East	West
	g	g	in.	in.	g	g	in.	in.	g	g	in.	in.
BASE MOTION	1.28	1.00	.14	1.17	1.97	2.40	.11	.88	2.7	2.6	1.70	.64
MEASURED RESPONSE												
North	1.35	1.25			1.28	1.22			1.30	1.37		
South	1.27	1.33			1.28	1.28			1.28	1.35		
Average	1.31	1.29	.46	.52	1.28	1.25	.54	.84	1.29	1.36	.44	.54
CALCULATED RESPONSE h=0	1.06	1.03	.48	.55	1.14	1.06	.80	1.00	1.06	1.03	.48	.55
h=0.02	1.08	1.04	.32	.44	1.14	1.12	.54	.74				

Mass accelerations were measured by accelerometers mounted on the north and south sides of the mass.

Table 1 Measured and Calculated Response to Simulated Earthquake Motions

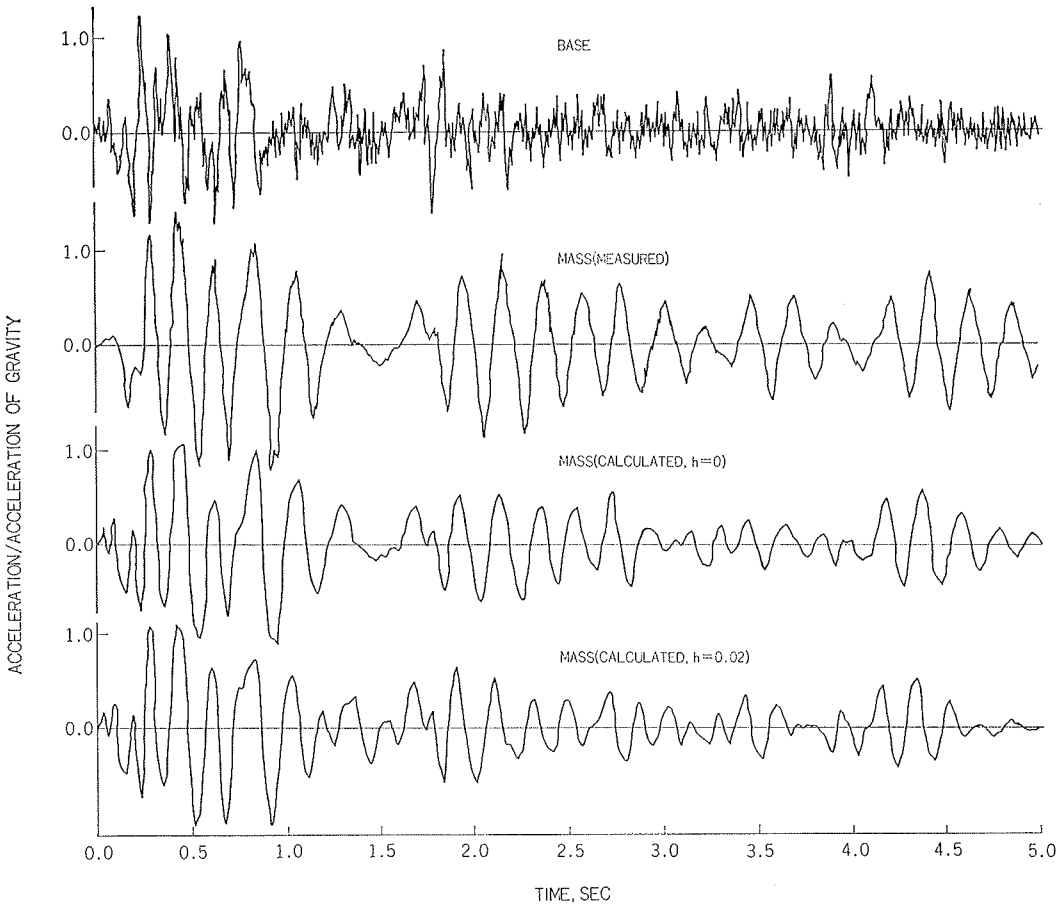

Fig. 4a Measured and Calculated Acceleration Response to Run 11

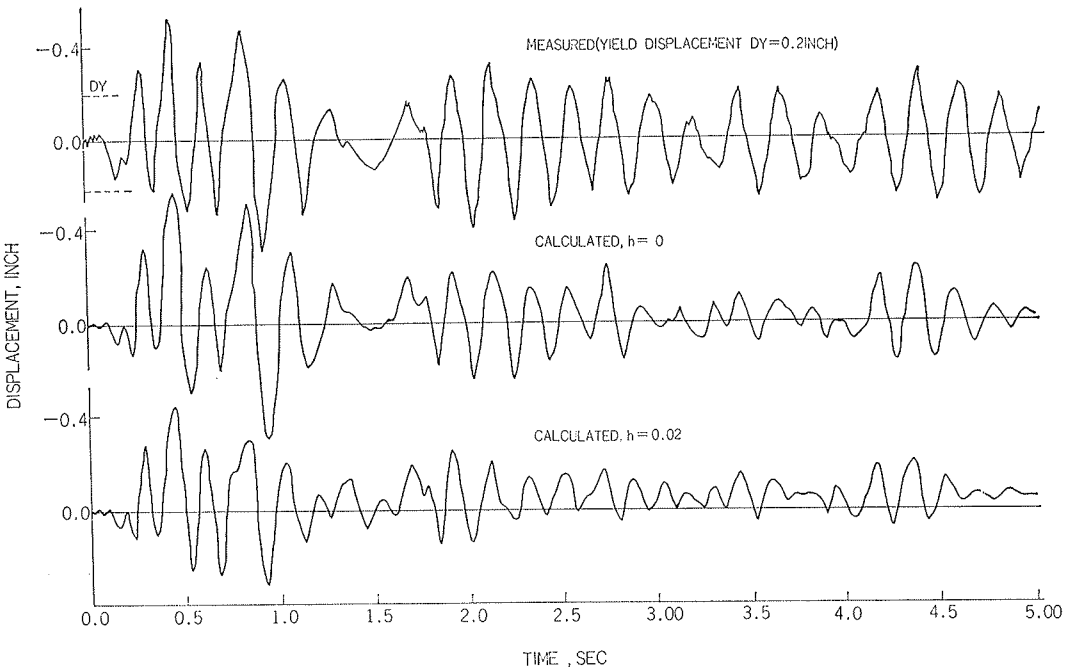

Fig. 4b Measured and Calculated Mass Displacement in Run 11

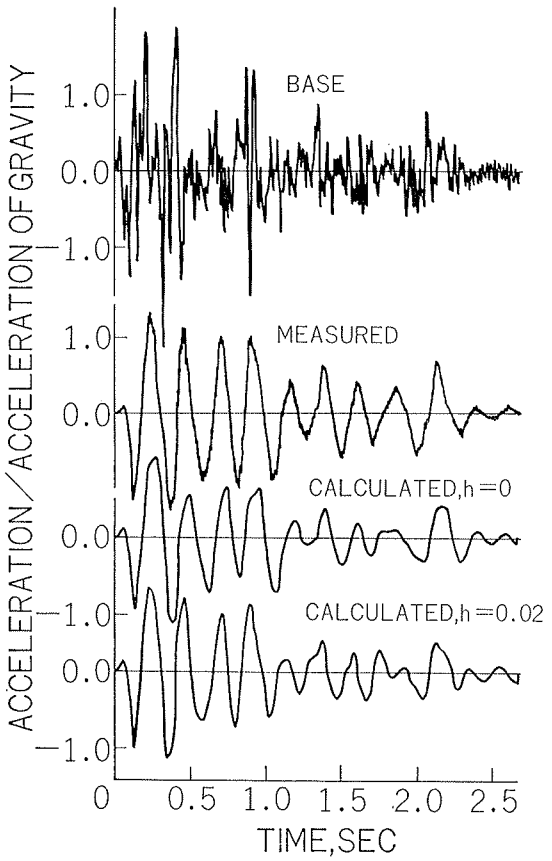

Fig. 5a Measured and Calculated Acceleration Response to Run 12

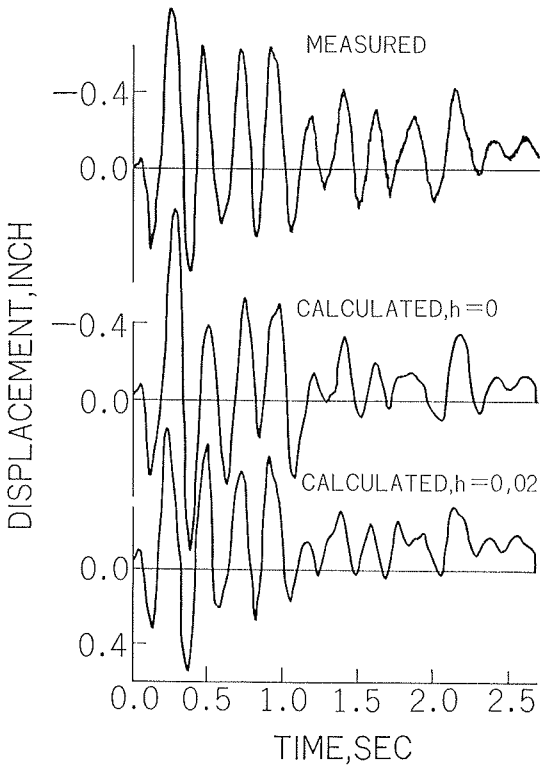

Fig. 5b Measured and Calculated Mass Displacement to Run 12

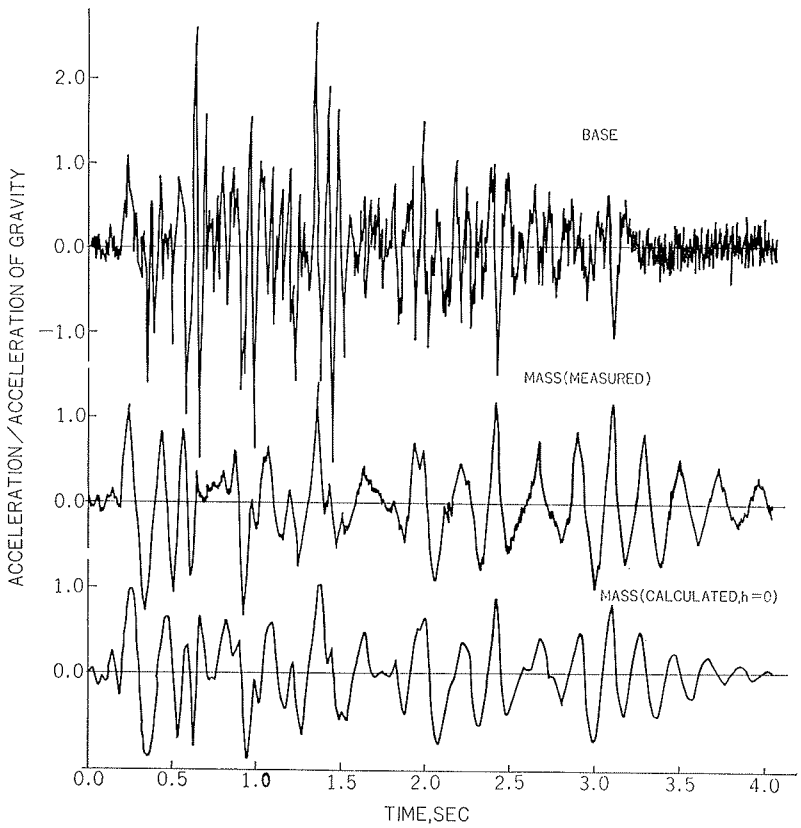

Fig. 6a Measured and Calculated Acceleration Response to Run 2′

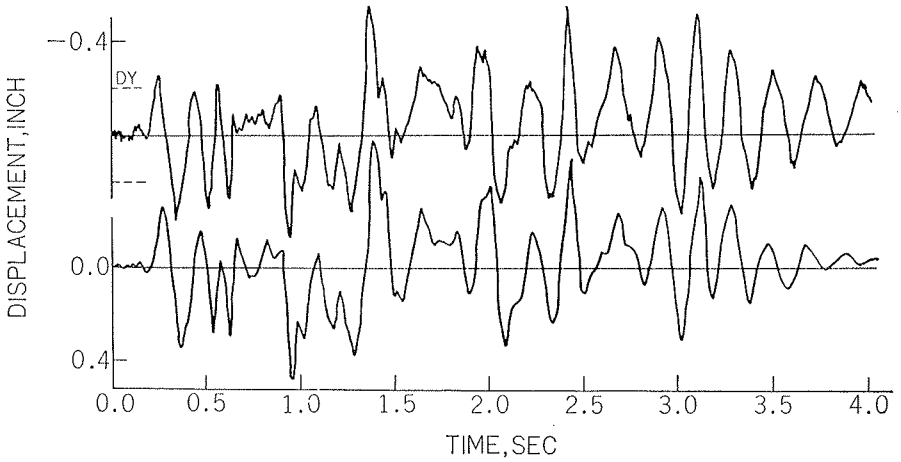

Fig. 6b Measured and Calculated Mass Displacement to Run 21

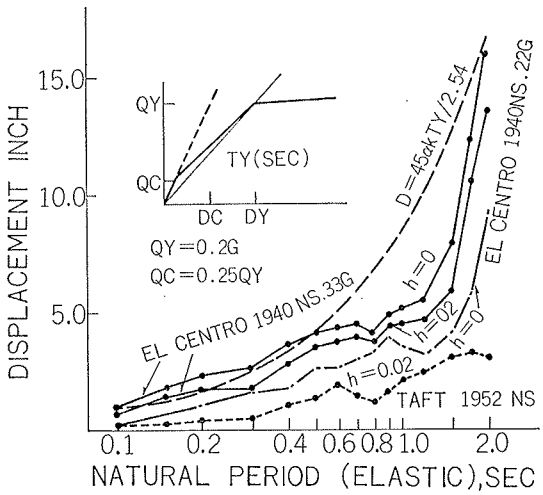

Fig. 7a Spectral Response

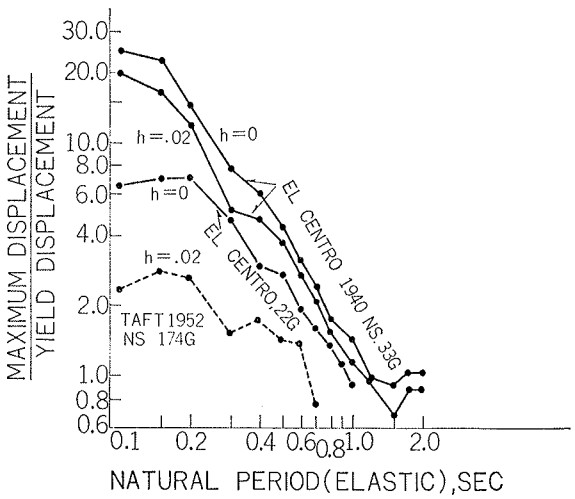

Fig. 7b Maximum Displacement/Yield Displacement